Philosophical Magazine
Publication details, including instructions for authors and subscription information:
http://www.tandfonline.com/loi/tphm20

Dielectric and magnetic permittivities of three new ceramic tungstates $MPr_2W_2O_{10}$ (M=Cd, Co, Mn)

Z. Kukuła [a], E. Tomaszewicz [b], S. Mazur [c], T. Groń [a], H. Duda [a], S. Pawlus [a], S.M. Kaczmarek [d], H. Fuks [d] & T. Mydlarz [e]

[a] University of Silesia, Institute of Physics, ul. Uniwersytecka 4, 40-007 Katowice, Poland

[b] West Pomeranian University of Technology, Department of Inorganic and Analytical Chemistry, Al. Piastów 42, 71-065 Szczecin, Poland

[c] The Henryk Niewodniczański Institute of Nuclear Physics, Polish Academy of Sciences, ul. Radzikowskiego 152, 31-342 Kraków, Poland

[d] West Pomeranian University of Technology, Institute of Physics, Al. Piastów 17, 70-310 Szczecin, Poland

[e] International Laboratory of High Magnetic Fields and Low Temperatures, ul. Gajowicka 95, 53-529 Wrocław, Poland

Published online: 10 Jul 2012.

To cite this article: Z. Kukuła , E. Tomaszewicz , S. Mazur , T. Groń , H. Duda , S. Pawlus , S.M. Kaczmarek , H. Fuks & T. Mydlarz (2012): Dielectric and magnetic permittivities of three new ceramic tungstates $MPr_2W_2O_{10}$ (M=Cd, Co, Mn), Philosophical Magazine, 92:33, 4167-4181

To link to this article: http://dx.doi.org/10.1080/14786435.2012.704427

Philosophical Magazine
Vol. 92, No. 33, 21 November 2012, 4167–4181

Taylor & Francis
Taylor & Francis Group

Dielectric and magnetic permittivities of three new ceramic tungstates $MPr_2W_2O_{10}$ (M = Cd, Co, Mn)

Z. Kukuła[a], E. Tomaszewicz[b], S. Mazur[c], T. Groń[a]*, H. Duda[a], S. Pawlus[a], S.M. Kaczmarek[d], H. Fuks[d] and T. Mydlarz[e]

[a]*University of Silesia, Institute of Physics, ul. Uniwersytecka 4, 40-007 Katowice, Poland;* [b]*West Pomeranian University of Technology, Department of Inorganic and Analytical Chemistry, Al. Piastów 42, 71-065 Szczecin, Poland;* [c]*The Henryk Niewodniczański Institute of Nuclear Physics, Polish Academy of Sciences, ul. Radzikowskiego 152, 31-342 Kraków, Poland;* [d]*West Pomeranian University of Technology, Institute of Physics, Al. Piastów 17, 70-310 Szczecin, Poland;* [e]*International Laboratory of High Magnetic Fields and Low Temperatures, ul. Gajowicka 95, 53-529 Wrocław, Poland*

(*Received 9 March 2012; final version received 7 June 2012*)

Broadband dielectric spectroscopy measurements revealed an anomalously large relative permittivity value ($\varepsilon_r = 884$) for $MnPr_2W_2O_{10}$, a smaller value ($\varepsilon_r = 156$) for $CoPr_2W_2O_{10}$ and the smallest value ($\varepsilon_r = 22$) for $CdPr_2W_2O_{10}$ at low frequency ($\nu = 0.1$ Hz) and above room temperature in the insulating and paramagnetic state. Below 273 K, the relative permittivity ($\varepsilon_r \sim 24$) did not depend significantly on frequency for all the tungstates under study. Electrical resistivity, thermoelectric power, electron paramagnetic resonance, magnetic susceptibility and magnetization provided experimental evidence that the studies tungstates were paramagnetic insulators with low *n*-type conduction. Only in the case of $MnPr_2W_2O_{10}$ was a ferrimagnetic order below 45 K observed. These effects are discussed within the framework of Maxwell–Wagner polarization, chemical covalent bonds and porosity mechanism.

Keywords: electrical properties; broadband dielectric spectroscopy; magnetic oxides

1. Introduction

Materials exhibiting a colossal dielectric constant (CDC) are of technical importance for applications such as multilayer capacitors, transducers, actuators, ferroelectric random access memory and display, microwave dielectric resonators and pyroelectric detector [1,2]. CDC behaviour has been observed in some high temperature superconductors as well as in ferroelectrics in a narrow temperature range close to the Curie temperature [3]. Usually, dipoles fluctuate by a static electric field, but these dipole fluctuations are unable to follow the electric field that generates the dielectric relaxation at high frequency. Therefore, wide band dielectric spectroscopy

*Corresponding author. Email: Tadeusz.Gron@us.edu.pl

ISSN 1478–6435 print/ISSN 1478–6443 online

http://dx.doi.org/10.1080/14786435.2012.704427
http://www.tandfonline.com

is a powerful tool to investigate the polarization mechanism of dielectric and ferroelectric materials [4].

Metal tungstates form a very large group of compounds and, owing to their interesting chemical, optical and structural properties, they are attractive materials for use in many important fields of technology. Tungstates of many *d*-electron metals, MWO_4, crystallize in a monoclinic wolframite-type structure with the space group $P2/c$ ($MnWO_4$ and $CoWO_4$) or $P2/b$ ($CdWO_4$) [5]. They have been successfully used in spectroscopic and radiometric devices and as heavy and fast scintillators [6–16]. Rare-earth metal tungstates (RE_2WO_6, where RE is the rare-earth metal), depending on a size of the RE^{3+} ionic radius and temperature, exhibit many structural types including a monoclinic structure with the space group $C2/c$ (where RE = Pr – Dy) [17]. They have found application as diode-pumped solid-state lasers, next generation lighting, in optical telecommunication, in lidar and in other applications requiring narrow spectral sources [18–20]. Our research group has examined the magnetic and electrical properties of RE_2WO_6 (RE = Nd, Sm, Eu, Gd, Dy, Ho and Er) in detail [21,22].

Novel *d*-electron and praseodymium tungstates with the general chemical formula $MPr_2W_2O_{10}$ (M = Cd, Co, Mn) have been successfully synthesized by a high-temperature solid-state reaction using MWO_4 and Pr_2WO_6 as the starting materials [23]. Their thermal and crystallographic properties have been described precisely in [23].

This paper reports on the electrical and magnetic properties of new $MPr_2W_2O_{10}$ tungstates (M = Cd, Co, Mn), which are important from the viewpoint of their potential dielectric and luminescence applications.

2. Experimental

2.1. *Preparation*

Pr_2WO_6 and MWO_4 (M = Cd, Co, Mn) were used as starting materials. Praseodymium tungstate was obtained by sintering Pr_6O_{11} (99.9%, Aldrich) with WO_3 (99.9%, Fluka) mixed in a 1:6 molar ratio and under thermal conditions described previously [23,24]. Divalent metal tungstates were prepared by heating an equimolar mixture of MnO (99.9%, Aldrich), $CoSO_4 \cdot 7H_2O$ (99.9%, Aldrich) or CdO (99.9%, Aldrich) with WO_3 under thermal conditions described previously [23,25–27]. MWO_4 and Pr_2WO_6 mixed in a 1:1 molar ratio were sintered in air and for 12-h periods at the following temperatures: 1173, 1223, 1273, 1298, 1323, 1348 and 1353 K. For better reactivity, the MWO_4/Pr_2WO_6 mixtures were ground in an agate mortar after each period of annealing. The samples obtained after the last heating stage were examined by a powder X-ray diffraction method. All diffraction lines in the XRD patterns were indexed with the orthorhombic-type structure. The prominent peaks correspond to [002], [032], [220], [221] and [212] lattice planes [23]. Sharp and very intense peaks indicated the crystalline nature of samples under study.

2.2. *Electrical and magnetic measurements*

Electrical resistivity was measured via a four-probe dc method using a semi-automatic bridge with an input impedance of 1.5 TΩ. The maximal error $\delta\rho/\rho$ was less than ±1%. Thermoelectric power was measured via a differential method using a temperature gradient ΔT of ~2 K. The accuracy of the thermopower value was estimated to be better than 3 μV/K. Dielectric measurements were carried out using pellets, polished and sputtered with (~80 nm) Ag electrodes in a frequency range from 10^{-1} to 10^{6} Hz on a Novocontrol Alpha Impedance analyzer. For electrical measurements, the powdered samples were compacted in disc form (10 mm in diameter and 1–2 mm thick) using a pressure of 1.5 GPa and then sintered at 473 K for 2 h.

Static (dc) magnetic susceptibility and magnetization isotherm measurements were performed using a Faraday-type Cahn RG automatic electrobalance up to 380 K and a vibrating sample magnetometer with a step motor in applied external fields up to 14 T, respectively. The dc susceptibilities as well as the magnetization isotherms were measured in zero-field-cooled (ZFC) mode. A fitting procedure of the Curie–Weiss law, eliminating the temperature-independent contribution (χ_0) [28] from the experimental susceptibility data, was used for determination of the magnetic parameters [29,30]. The fitted reciprocal magnetic susceptibility $1/(\chi_\sigma - \chi_0)$ is marked in red. This dependence is approximated by the red straight line $(T-\theta)/C_\sigma$, which intersects the temperature axis at $T=\theta$ and its inclination equals $1/C_\sigma$.

2.3. *EPR measurements*

EPR measurements were performed with a conventional X-band Bruker ELEXSYS E500 CW spectrometer operating at 9.5 GHz with 100 kHz magnetic field modulation. The temperature dependence of the EPR spectra was registered in the 3.28–260 K temperature range controlled by an Oxford flow cryostat.

3. Results and discussion

3.1. *Electrical properties*

The results for electrical resistivity (ρ), thermopower (S) and relative dielectric permittivity (ε_r) measurements of $MPr_2W_2O_{10}$ (M = Cd, Co, Mn) are collated in Table 1 and illustrated in Figures 1–5. All tungstates under study are insulators with an electrical resistivity of 10^8 Ωm. In Figure 1, $\rho(T)$ exhibits a weak temperature dependence but only for $MnPr_2W_2O_{10}$ is a thermally activated conduction of the Arrhenius-type above 400 K observed. The sign of thermopower is negative for all studies tungstates (Figure 2), suggesting that the residual electrical *n*-type conduction appears to be associated with an excess of oxygen vacancies.

The variation in relative dielectric constants (ε_r) and loss tangent (tan δ) at 173, 193, 223, 273, 323 and 373 K with frequency (10^{-1}–10^{6} Hz) are shown in Figure 3 for

Table 1. Electrical and magnetic parameters of $MPr_2W_2O_{10}$ tungstates (M = Cd, Co, Mn): C_σ is the Curie constant, μ_{eff} is the effective magnetic moment, θ is the Curie–Weiss temperature, χ_0 is the temperature-independent contribution of magnetic susceptibility, ρ is the electrical resistivity at 300 K, S is the thermoelectric power at 300 K and ε_r is the relative electrical permittivity at 373 K and with frequency $\nu = 0.1$ Hz.

	Magnetic measurements				Electrical measurements		
Compound	C_σ (K · cm^3/g)	μ_{eff} (μ_B/f.u.)	θ (K)	χ_0 (cm^3/g)	$\rho_{(300\,K)}$ (Ωm)	$S_{(300\,K)}$ (μV/K)	$\varepsilon_{r(373\,K)}$
$CdPr_2W_2O_{10}$	$3.196 \cdot 10^{-3}$	4.86	−26.8	$5.931 \cdot 10^{-6}$	$1.64 \cdot 10^8$	−321	22
$CoPr_2W_2O_{10}$	$5.34 \cdot 10^{-3}$	6.09	−40.8	$3.701 \cdot 10^{-6}$	$2.45 \cdot 10^8$	−374	156
$MnPr_2W_2O_{10}$	$5.274 \cdot 10^{-2}$	6.04	−16.0	$4.581 \cdot 10^{-6}$	$3.14 \cdot 10^8$	−269	884

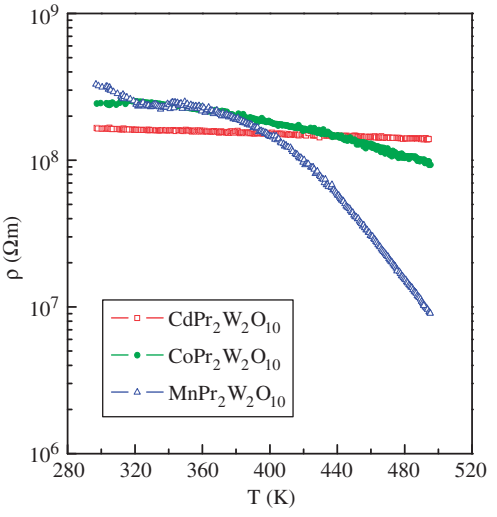

Figure 1. Electrical resistivity ρ versus temperature T for $MPr_2W_2O_{10}$ tungstates (M = Cd, Co, Mn).

$CdPr_2W_2O_{10}$, in Figure 4 for $CoPr_2W_2O_{10}$ and in Figure 5 for $MnPr_2W_2O_{10}$. In the case of $CdPr_2W_2O_{10}$, ε_r does not exceed a value of 24. It decreases slightly with frequency but remains almost constant with temperature, which is normal behaviour for dielectric/ferroelectric materials [2]. The loss tangent of this compound is close to zero for higher frequencies but a slight reduction ($\delta < 5^\circ$) is visible for low frequencies (inset to Figure 3). Such features of permittivity are expected, since Cd^{2+} ions have the 3*d*-shell filled, but Pr^{3+} ions have the 4*f*-shell screened. In the case of $CoPr_2W_2O_{10}$ and $MnPr_2W_2O_{10}$, both $\varepsilon_r(\nu)$ and tan $\delta(\nu)$ are dramatically changed below 10^2 Hz. At 10^{-1} Hz, ε_r reaches values of 156 for $CoPr_2W_2O_{10}$ (Figure 4) and 884 for $MnPr_2W_2O_{10}$ (Figure 5), which are far from saturation. Such a large value for relative permittivity strongly depends on the type of 3*d* ion, but not on the type of

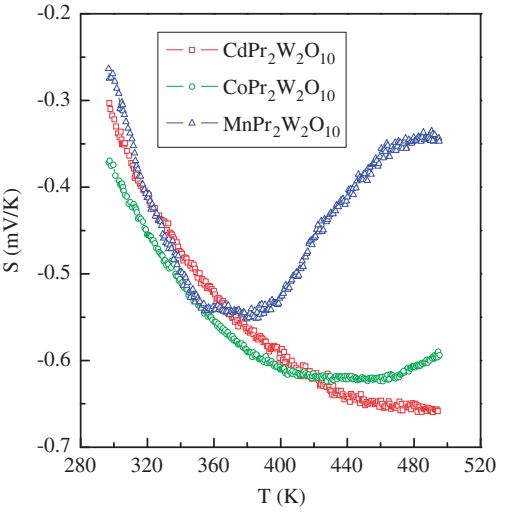

Figure 2. Thermoelectric power S versus temperature T for $MPr_2W_2O_{10}$ tungstates (M = Cd, Co, Mn).

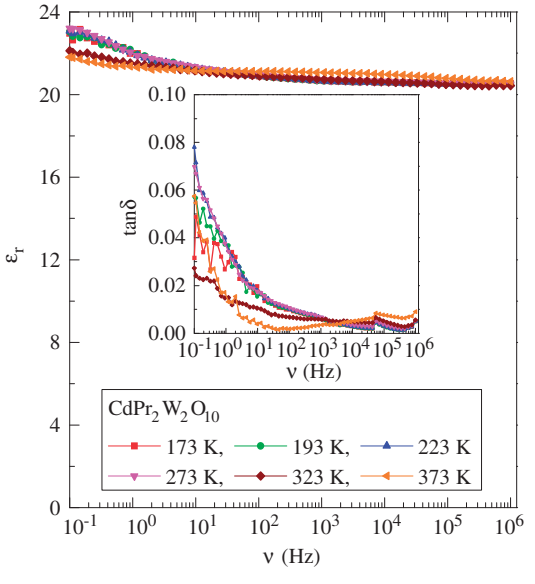

Figure 3. Relative permittivity ε_r and loss tangent tan δ (inset) of $CdPr_2W_2O_{10}$ at frequencies ν of 173, 193, 223, 273, 323 and 373.

4*f* ion. The Co^{2+} and Mn^{2+} ions have both the unfilled and unscreened 3*d*-shells. They only differ in a number of unpaired electrons.

This rapid increase in ε_r with increasing temperature and/or decreasing frequency has been observed in some ferroelectric materials and can results from a Maxwell–Wagner-type effect (MW) [1,31–33]. MW relaxations are non-intrinsic and can be

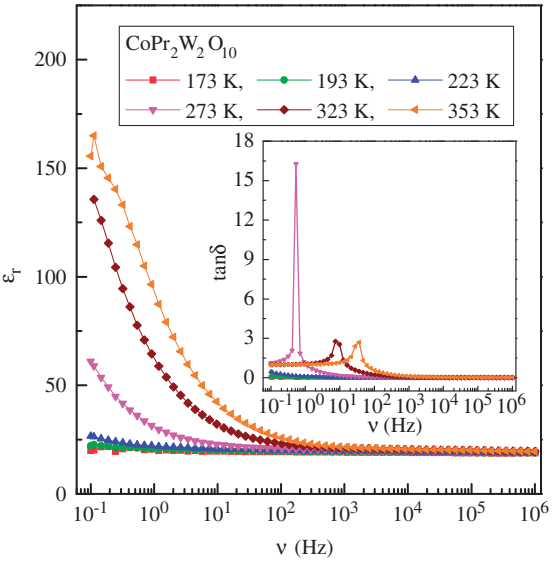

Figure 4. Relative permittivity ε_r and loss tangent tan δ (inset) of $CoPr_2W_2O_{10}$ at frequencies ν of 173, 193, 223, 273, 323 and 353.

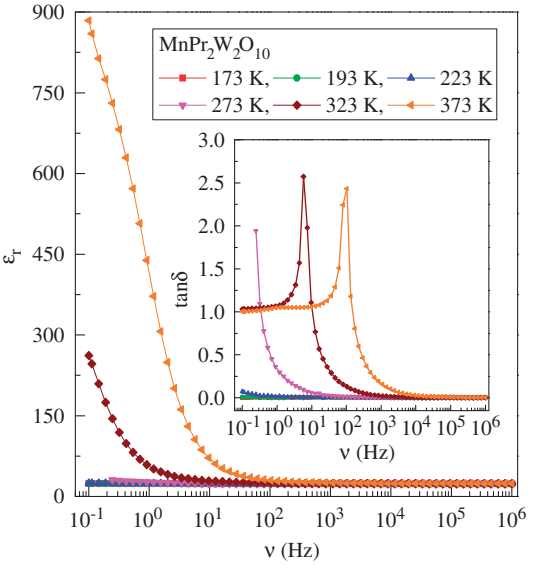

Figure 5. Relative permittivity ε_r and loss tangent tan δ (inset) of $MnPr_2W_2O_{10}$ at frequencies ν of 173, 193, 223, 273, 323 and 373.

described by an equivalent electric circuit consisting of the bulk contribution from the sample, connected in series to a parallel resistance–capacitance (RC) circuit, with R and C being much higher that the corresponding bulk quantities. This region with a high resistance in the sample can arise from insulating depletion layers at the

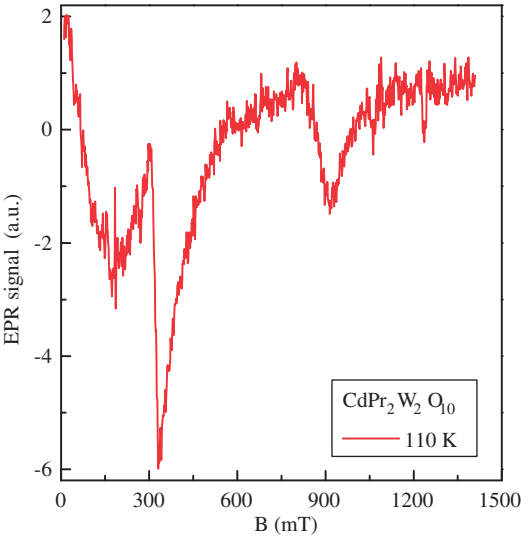

Figure 6. First derivative EPR signal of $CdPr_2W_2O_{10}$ measured at 110 K.

metal-to-sample contacts or other type of internal barriers. At high frequencies and/or low temperatures, the layer capacitance becomes shortened and only bulk behaviour is detected. However, with increasing temperature and/or decreasing frequency, the high capacitance of these insulating layers leads to the detection of a markedly increasing value of ε_r [33].

Large values of $\tan\delta$ at low frequencies may suggest that both tungstates (insets to Figures 4 and 5) show relaxation behaviour above 273 K. In general, the tungstates under study have one feature in common: below 273 K, the relative permittivity is small ($\varepsilon_r \sim 24$) and does not depend significantly on frequency. A reason of this low value of ε_r may be the highly chemical covalent bonds with a complex structure from one side and no local electrical conduction from the other [34]. Also, the presence of porosity in these materials can result in a low dielectric constant, since air has the lowest dielectric constant [2]. However, the average experimental density ($\sim$7.00 g/cm^3) [23] is a smaller than the theoretical value ($\sim$7.03 g/cm^3) [23] what means the porosity level for the compounds under study ($\sim$0.43%) should not affect the main effect.

3.2. *EPR spectra*

The temperature evolution of the first derivative EPR spectra for $CdPr_2W_2O_{10}$, $CoPr_2W_2O_{10}$ and $MnPr_2W_2O_{10}$ tungstates are presented in Figures 6, 7 and 9, respectively. The spectrum of $CdPr_2W_2O_{10}$ does not contain any signal from the paramagnetic centre. The intensity and shape of EPR signal, presented in Figure 6, do not significantly change on temperature and magnetic field and describes only the chamber effects. This is clear, since Cd^{2+} and W^{6+} as nonmagnetic ions give no EPR signal, as with the Pr^{3+} ion, being a non-Kramer's ion with a high separation between ground and excited states.

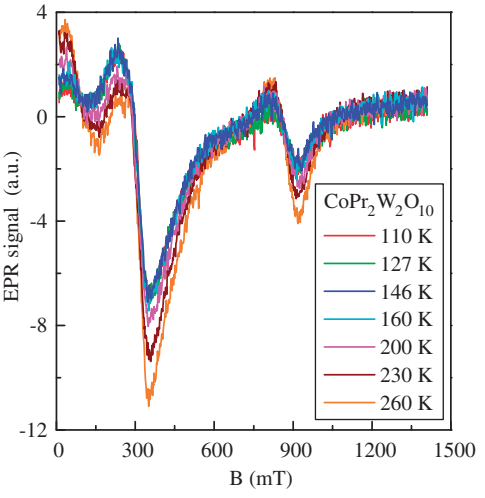

Figure 7. First derivative EPR signals of $CoPr_2W_2O_{10}$ measured at different temperatures.

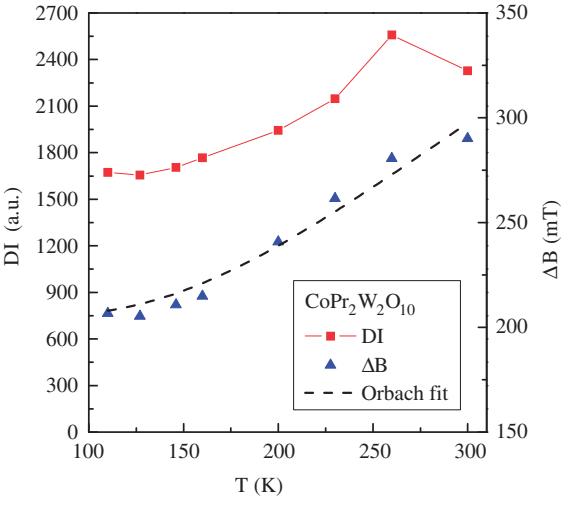

Figure 8. EPR susceptibility as a double integration of the spectrum *DI* and the linewidth of the EPR signal ΔB versus temperature T for $CoPr_2W_2O_{10}$. The dashed line is for an Orbach curve fitted to the experimental data.

The EPR spectra of $CoPr_2W_2O_{10}$ (Figure 7) were registered at temperatures between 110 and 260 K. They show one wide and asymmetric line attributed to the Co^{2+} ions with spin $S = 3/2$. A similar effect was observed for $CoGd_4W_3O_{16}$ [35]. EPR susceptibility of $CoPr_2W_2O_{10}$ as a double integration of the spectrum *DI* increases with increasing temperature (Figure 8). This unusual behaviour could be explained by the increasing role of the excited states, giving a significant magnetic

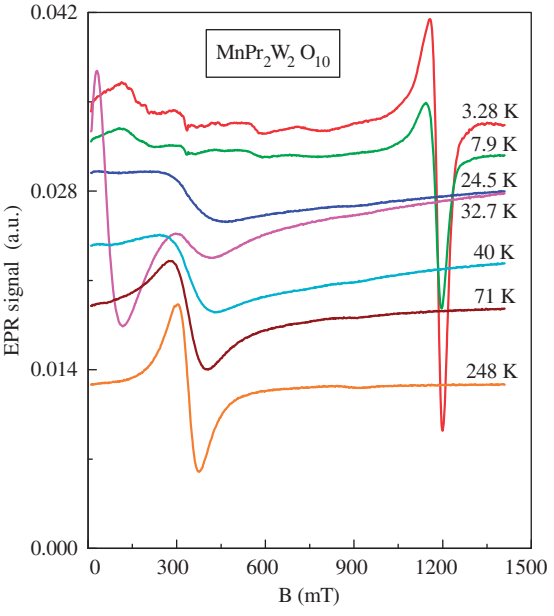

Figure 9. First derivative EPR signals of $MnPr_2W_2O_{10}$ measured at different temperatures.

component to the whole signal. This suggestion seems to be reasonable if we notice that the linewidth of the EPR signal ΔB increases with temperature (Figure 8). It suggests the presence of specific phonon, Raman and Orbach processes involved in the spin–lattice relaxation phenomenon [36]. This process enables the employment of excited paramagnetic states to the resonance phenomenon. In this case, the following relation should be fulfilled: $\Delta B = \Delta B_0 + Ae^{-W/kT}$, where ΔB_0 is the residual linewidth, A is the experimental parameter, k is the Boltzmann's constant and W is the energy difference between ground and first excited state. The result of fitting (dashed line in Figure 8) gives the following values: $\Delta B_0 = 205\,\text{mT}$, $W/k = 601\,\text{K}$.

Figure 9 presents the EPR signal of $MnPr_2W_2O_{10}$ measured at different temperatures. As one can see, the resonance spectrum is rather complex and undergoes a significant temperature evolution. A characteristic feature of the spectra is the appearance of a narrow and intense EPR line at temperatures close to 33 K in a low magnetic field. This curiosity may be a result of local destabilization of the ferrimagnetic order, leading consequently to the appearance of a resonance signal accompanying ferromagnetic clusters. Generally, we expect that the shape of the observed EPR signal is a superposition of five narrow lines of fine interaction ($S = 5/2$) and six hyperfine lines ($I = 5/2$) of Mn^{2+} paramagnetic centres. As the manganese system in this material is very dense, the width of the component lines becomes large due to significant dipole–dipole and exchange interactions between magnetic entities, and, as a result, the observed magnetic signal does not allow recognize fine and hyperfine constituents. The close Lorentzian shape of the composite lines suggests that the exchange interactions dominate in the manganese system. EPR susceptibility as a double integration of the spectrum DI versus temperature is shown in Figure 10.

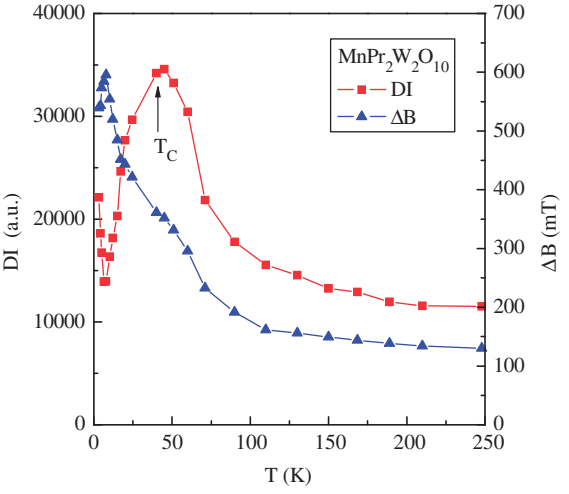

Figure 10. EPR susceptibility as a double integration of the spectrum DI and the linewidth of the EPR signal ΔB versus temperature T for $MnPr_2W_2O_{10}$. The Curie temperature T_C is marked by an arrow.

As can be seen, the points of the $DI(T)$ relation follow the Curie-Weiss law at mainly higher temperatures, while, below 45 K, a significant change in inclination is revealed. This behaviour is typical for ferrimagnetic interactions dominating in magnetic system. A similar effect was observed in the temperature relation of the linewidth ΔB (Figure 10), where the main EPR line is centred at 350 mT.

3.3. *Magnetic properties*

The temperature dependence of magnetic susceptibility $\chi(T)$ and its reverse $1/\chi(T)$ showed paramagnetic behaviour in the temperature range 5–370 K both for $CdPr_2W_2O_{10}$ (Figure 11) and $CoPr_2W_2O_{10}$ (Figure 12). In case of $MnPr_2W_2O_{10}$ (Figure 13), a peak on the $\chi(T)$ curve at $T_C = 45$ K and the deviation of the $1/\chi(T)$ curve downward from its linear portion are characteristic for the ferrimagnetic coupling of magnetic moments. On the other hand, all tungstates under study show negative values for the paramagnetic Curie–Weiss temperature, θ, and positive values for the temperature-independent contribution of magnetic susceptibility, χ_0, (Table 1). This may indicate antiferromagnetic short-range interactions from one side and temperature-independent contributions of orbital and Landau diamagnetism, Pauli and Van Vleck paramagnetism among others from the other side, as they cannot be separated. Because the studies tungstates are insulators, the Landau and Pauli contributions can be neglected. The relative magnetic permittivity (μ_r) of all examined tungstates, estimated from the equation: $\mu_r = d\chi + 1$, where d is the density, does not exceed a value of 1.007, characteristic for paramagnets, and is weakly dependent on temperature.

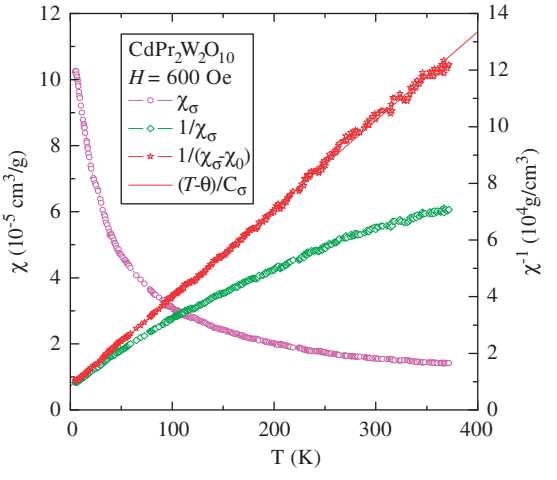

Figure 11. Magnetic susceptibility χ and χ^{-1} of $CdPr_2W_2O_{10}$ with temperature T recorded at magnetic field $H = 600$ Oe. The solid (red) line indicates Curie–Weiss behaviour.

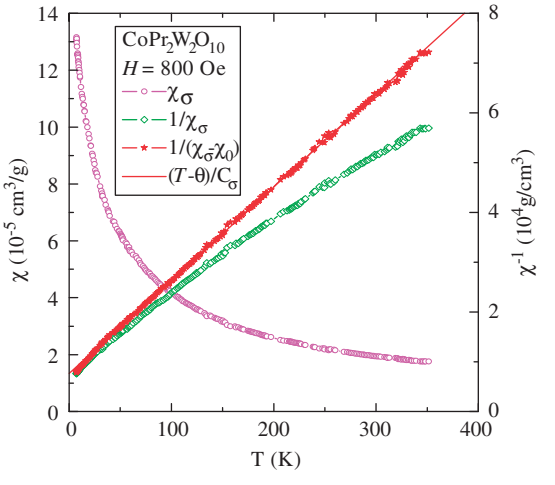

Figure 12. Magnetic susceptibility χ and χ^{-1} of $CoPr_2W_2O_{10}$ with temperature T recorded at magnetic field $H = 800$ Oe. The solid (red) line indicates Curie–Weiss behaviour.

The experimental effective magnetic moments estimated from the equation: $\mu_{\text{eff}} = 2.83\sqrt{MC_\sigma}$, where M is the molar mass and C_σ is the Curie constant are presented in Table 1. For $CdPr_2W_2O_{10}$ and $CoPr_2W_2O_{10}$, these moments are quite close to the theoretical values calculated from equations $p_{\text{eff}} = \sqrt{2}p_{\text{Pr}}$ and $p_{\text{eff}} = \sqrt{p_{\text{Co}}^2 + 2p_{\text{Pr}}^2}$ [35], respectively, where $p = g\sqrt{J(J+1)}$ is the effective number of Bohr magnetons [28], J is the effective angular momentum and g is the Landé factor. Because JLS coupling works for the screened RE 4f-shell, but not for the

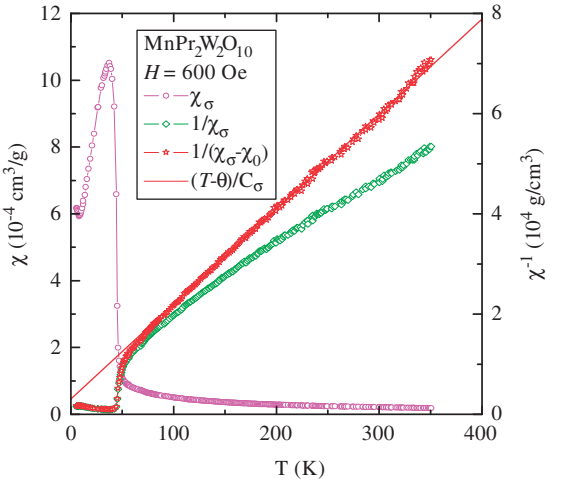

Figure 13. Magnetic susceptibility χ and χ^{-1} of $MnPr_2W_2O_{10}$ with temperature T recorded at magnetic field $H = 600$ Oe. The solid (red) line indicates Curie–Weiss behaviour.

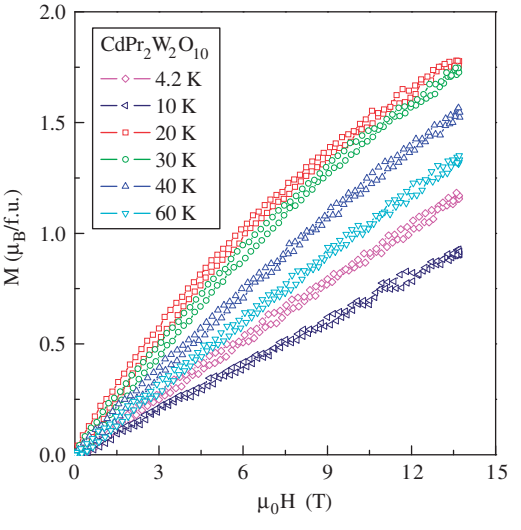

Figure 14. Magnetization M of $CdPr_2W_2O_{10}$ with magnetic field H at 4.2, 10, 20, 30, 40 and 60 K.

unscreened TM 3*d*-shell [35], for the p_{eff} calculations, only effective spins of 3/2 of Co and 5/2 of Mn ions were taken from the EPR experiment. In the case of $MnPr_2W_2O_{10}$, the effective magnetic moment is quite close to the spin-only value of the Mn^{2+} ion, for which $g = 1.995$ was estimated from the deconvolution of the first derivative of EPR absorption made using superposition of five Gaussian shape lines.

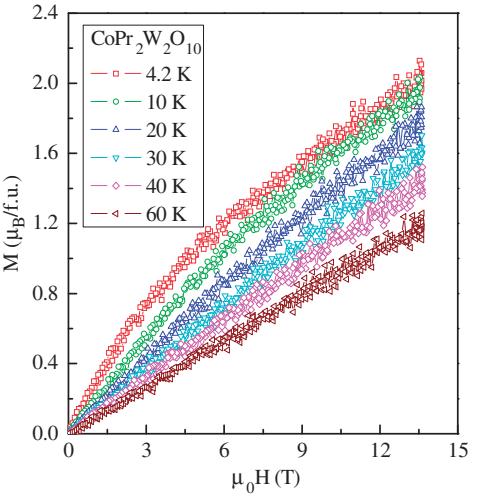

Figure 15. Magnetization M of $CoPr_2W_2O_{10}$ with magnetic field H at 4.2, 10, 20, 30, 40 and 60 K.

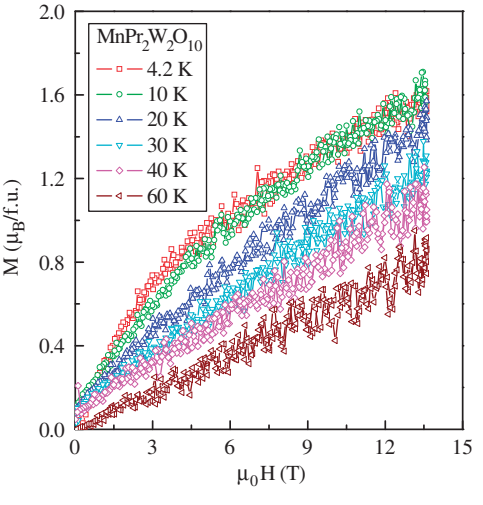

Figure 16. Magnetization M of $MnPr_2W_2O_{10}$ with magnetic field H at 4.2, 10, 20, 30, 40 and 60 K.

It gives a value of magnetic moment for Mn^{2+} as high as 5.91 μ_B/f.u. which is comparable with the value derived from magnetization measurements, i.e. 6.3 μ_B/f.u.

Magnetic isotherms for $CdPr_2W_2O_{10}$ (Figure 14), $CoPr_2W_2O_{10}$ (Figure 15) and $MnPr_2W_2O_{10}$ (Figure 16) measured up to 14 T are characteristic of the universal

Brillouin function, indicating paramagnetic response [37]. Their shape suggests that these tungstates are far from saturation magnetization.

4. Conclusions

We have investigated the electrical and magnetic properties of powdered $MPr_2W_2O_{10}$ tungstates (M = Cd, Co, Mn). The results showed a colossal relative permittivity for $MnPr_2W_2O_{10}$ at 0.1 Hz in the insulating and paramagnetic state above 273 K. Below this temperature, all tungstates under study had a low value of the dielectric constant $\varepsilon_r \sim 24$. The results also showed that the $MPr_2W_2O_{10}$ tungstates (M = Cd, Co, Mn) are paramagnetic insulators with the exception of $MnPr_2W_2O_{10}$, which reveals the ferrimagnetic order below 45 K. The main conclusion is that only those ions which have unscreened electrons on the unfilled shells are responsible for the colossal dielectric effect.

Acknowledgements

This work was partly supported by Ministry of Scientific Research and Information Technology (Poland). The authors are very grateful to Professor D. Skrzypek from the Institute of Physics of the University of Silesia in Katowice for her helpful discussion.

References

[1] P. Lunkenheimer, V. Bobnar, A.V. Pronin, A.I. Ritus, A.A. Volkov and A. Loidl, Chem. Phys. Rev. B 66 (2002) p.052105.
[2] P.C. Joshi, S.O. Ryu, S. Tirumala and S.B. Desu, MRS Proceedings 493 (1997) p.215.
[3] G. Chern, L.R. Song and J.B. Shi, Physica C 253 (1995) p.97.
[4] T. Teranishi, T. Hoshina and T. Tsurumi, Mater. Sci. Eng. B 161 (2009) p.55.
[5] A.W. Sleight, Acta Crystallogr. B 28 (1972) p.2899.
[6] L. Nagornaya, G. Onyshchenko, E. Pirogov, N. Starzhinkiy, I. Tupitsyna, V. Ryzhikov, Yu. Galich, Yu. Vostretsov, S. Galkin and E. Voronkin, Nucl. Instrum. Methods Phys. Res. A 537 (2005) p.163.
[7] N. Klassen, S. Shmurak, B. Red'kin, B. Ille, M. Lebeau, P. Lecoq and M. Schneegans, Nucl. Instrum. Methods Phys. Res. A 486 (2002) p.431.
[8] V. Ryzhikov, L. Nagornaya, V. Volkov, V. Chernikov and O. Zelenskaya, Nucl. Instrum. Methods Phys. Res. A 486 (2002) p.156.
[9] D. Brown, R.H. Olsher, Y. Eisen and J.F. Rodriguez, Nucl. Instrum. Methods Phys. Res. A 373 (1996) p.139.
[10] K. Tanaka, N. Shirai, I. Sugiyama and R. Nakata, Nucl. Instrum. Methods Phys. Res. B 121 (1997) p.404.
[11] V.G. Bodnar, S.F. Burachas, K.A. Katrunov, V.P. Martinov, V.D. Ryzhikov, V.I. Manko, H.H. Gutbrod and G. Tamulaitis, Nucl. Instrum. Methods Phys. Res. A 411 (1998) p.376.
[12] L. Nagornaya, S. Burachas, Yu. Vostretsov, V. Martynov and V. Ryzhikov, J. Cryst. Growth 198/199 (1999) p.877.
[13] H. Lotem and Z. Burshtein, Opt. Lett. 12 (1987) p.561.
[14] M. Kobayashi, Y. Usuki, M. Ishii and M. Itoh, Radiat. Meas. 38 (2004) p.375.
[15] O. Chukova, S. Nedilko, Z. Moroz and M. Pashkovskyi, J. Lumin. 102/103 (2003) p.498.

[16] H. Shang, Y. Wang, B. Milbrath, M. Bliss and G. Cao, J. Lumin. 121 (2006) p.527.
[17] A.A. Evdokimov, V.A. Efremov and V.K. Trunov, *Compounds of the Rare Earth Elements: Molybdates and Tungstates*, Nauka, Moscow, 1991 (in Russian).
[18] G. Boulon, Opt. Mater. 34 (2012) p.499.
[19] M.F. Joubert, Opt. Mater. 11 (1999) p.181.
[20] A. Rapaport, J. Milinez, M. Bass, A. Cassanho and H. Jenssen, J. Display Technol. 2 (2006) p.68.
[21] P. Urbanowicz, E. Tomaszewicz, T. Groń, H. Duda, A.W. Pacyna and T. Mydlarz, Physica B 404 (2009) p.2213.
[22] T. Groń, E. Tomaszewicz, P. Urbanowicz, H. Duda and T. Mydlarz, Acta Phys. Pol. A 119 (2011) p.708.
[23] E. Tomaszewicz, J. Therm. Anal. Cal. 93 (2008) p.711.
[24] S.M. Kaczmarek, E. Tomaszewicz, D. Moszyński, A. Jasik and G. Leniec, Mater. Chem. Phys. 124 (2010) p.646.
[25] E. Tomaszewicz, Thermochim. Acta 447 (2006) p.69.
[26] E. Tomaszewicz, J. Therm. Anal. Cal. 90 (2007) p.255.
[27] E. Tomaszewicz and S.M. Kaczmarek, Rev. Adv. Mater. Sci. 23 (2010) p.88.
[28] A.H. Morrish, *Physical Principles of Magnetism*, Wiley, New York, 1965.
[29] T. Groń, E. Malicka and A.W. Pacyna, Physica B 404 (2009) p.3554.
[30] T. Groń, A.W. Pacyna and E. Malicka, Solid State Phenom. 170 (2011) p.213.
[31] S. Krohns, P. Lunkenheimer, Ch. Kant, A.V. Pronin, H.B. Brom, A.A. Nugroho, M. Diantoro and A. Loidl, Appl. Phys. Lett. 94 (2009) p.122903.
[32] P. Lunkenheimer, S. Krohns, S. Riegg, S. g. Ebbinghaus, A. Reller and A. Loidl, Eur. Phys. J. Special Topics 180 (2009) p.61.
[33] J.J. Sebald, S. Krohns, P. Lunkenheimer, S.G. Ebbinghaus, S. Riegg, A. Reller and A. Loidl, Solid State Commun. 150 (2010) p.857.
[34] S. Seraji, Y. Wu, M. Forbess, S.J. Limmer, T. Chou and G. Cao, Adv. Mater. 12 (2000) p.1695.
[35] P. Urbanowicz, E. Tomaszewicz, T. Groń, H. Duda, A.W. Pacyna, T. Mydlarz, H. Fuks, S.M. Kaczmarek and J. Krok-Kowalski, J. Phys. Chem. Solids 72 (2011) p.891.
[36] H. Fuks, S.M. Kaczmarek, G. Leniec, L. Macalik, B. Macalik and J. Hanuza, Opt. Mater. 402 (2010) p.1560.
[37] S.A. Majetich, J.O. Artman, M.E. McHenry, N.T. Nuhfer and S.W. Stanley, Phys. Rev. B 48 (1993) p.16845.